Experimental study on gyroscopic effect of rotating rotor and wind heading angle on floating wind turbine responses

Int. J. Environ. Sci. Technol.
DOI 10.1007/s13762-017-1519-4

ORIGINAL PAPER

Experimental study on gyroscopic effect of rotating rotor and wind heading angle on floating wind turbine responses

S. Bahramiasl[1] · M. Abbaspour[1] · M. Karimirad[2]

Received: 22 October 2016 / Revised: 4 March 2017 / Accepted: 15 July 2017

Abstract Limited fossil resources, daily increasing rate of demand for energy and the environmental pollution fact have made people revert to renewable sources of energy as a solution. One type of renewable energy is offshore wind energy which has high potential without any sound and visual noises. Recently, a lot of researchers have carried out on the issue of offshore wind turbine. Because of incapability of most of software programs to simulate gyroscopic effect of rotating rotors, in this articles a significant effort has been made to fabricate and test an offshore wind turbine under different rotor rotation velocities and different heading angle of wind so as to obtain the effects of these parameters on structure responses. Study on the response of a wind turbine under environmental loads has had a notable importance due to the fact that structure behavior can strongly affect procedure of modeling and optimizing wind turbine structures. On the other hand, frequency-domain structural response of a wind turbine can also make engineers be informed about of appropriate mooring system for a special environmental condition. Consequently, it has been observed that increasing the rotor rotation velocity leads the peak of spectrums shift to a higher frequency due to the gyroscopic effect appeared as a damping term, and changing heading angle of wind may lead to a change in heave and pitch amplitudes in the time domain response, and heave, sway and surge motion in frequency response.

Keywords Offshore wind turbine · Experimental study · Gyroscopic effect · Rotor rotation · Frequency domain

Editorial responsibility: Necip Atar.

✉ M. Karimirad
madjid.karimirad@qub.ac.uk

[1] School of Mechanical Engineering, Sharif University of Technology, Tehran, Iran

[2] Queen's University Belfast (QUB), Belfast BT95AG, United Kingdom

Introduction

Nowadays, environmental pollution of fossil fuels has leaded many researchers to focus on renewable energy. Among different types of renewable energy, offshore wind has drawn attention of many researchers to itself due to high potential of wind in offshore areas, whereas it has no acoustic and optical noises. Offshore wind energy has been found as an appropriate substitution to fulfill this demand. It has conducted a lot of studies on the FOWT (Floating Offshore Wind Turbine) responses in a variety of sea conditions. Experimental investigation has been conducted on a TLP FOWT with conical substructure moored by a spring tension leg, subjected to the wave, wind and rotor rotating loads (Shin 2011). The RAOs of structure motions have been obtained and discussed. Their results have shown that the new concept has had a good stability and decent responses. Three types of FOWT, TLP, spar and semisubmersible, have studied by a numerical time domain approach which has been used for a fully coupled dynamic analysis of FOWTs. Also, the mooring system of semisubmersible equipped with six and eight mooring lines has been investigated, and the platform rotations have been compared along with motions (Bagbanci 2011). The "Hywind" turbine has been modeled by FAST code and the results have been validated by experimental testing the model. Also, the FAST ADAMS code has been used for calculating the aerodynamic loads and WAMIT code has

Published online: 03 October 2017

been used in order to calculate hydrodynamic loads (Jonkman 2007; Browning et al. 2014). A TLP and a spar type of FOWT have been modeled and tested experimentally (Naqvi 2012). Preliminarily aerodynamic interaction of flow and pitch structure responses has been studied by using the time averaged unsteady Reynolds averaged Navier–Stokes (URANS) method (Matha et al. 2011). Gyroscopic effect of a FOWT has been investigated by driving the equation of motion and calculating and adding gyroscopic damping in the equation (Fujiwara et al. 2011). A FOWT with a revolving disk on its top has been tested and the responses of the platform with the rotating disk and without it have been analyzed in frequency domain. Also, the numerical studies have shown that the rotating disk would induce an extra peak in yaw motion and shift peak of surge and pitch motion to a higher frequency. Effect of additional mooring chain on the response of a TLP FOWT model with cylindrical and square support has been studied, and the responses of two different structures have been obtained and discussed (Ren et al. 2012a, b). The results have represented that the additional mooring would play an active role in reducing surge motion, surge acceleration and tension leg force responses of the structure.

The effect of gyroscopic couples on the response of a semisubmersible FOWT has been investigated (Blusseau and Patel 2012). The equations of motions in 6 DOFs (Degree Of Freedom) have been formulated in frequency domain and aerodynamic loads have been added and effect of gyroscopic couples on the structure responses has been studied.

Dynamic response of a TLP FOWT has been numerically investigated under environmental loads (Ebrahimi et al. 2014). The code has taken off-diagonal component of stiffness, damping and mass matrices into account so as to study the coupling of surge and pitch motions. For validating the numerical results, the 1:135 scaled-down model has been tested in the laboratory. A 1:50 scaled model of semisubmersible FOWT has been tested and investigated in the wave-wind flume and the dynamic motions of the structure have been analyzed (Hsu et al. 2016). Actually, a solid disk has been used for simulating thrust force on the wind turbine and natural frequency and damping coefficient have been obtained by free decay test. A unified methodology for testing FROUDE scale models of FOWTs has been presented and some methods have been suggested for fabricating a high quality low turbulence FOWT in a wave tank to simplify simultaneous application of wind and waves to the model (Martin et al. 2012). A scaled model of NREL (National Renewable Laboratory) 5 MW wind turbine Matha (2010) has been tested and studied on three different platforms TLP, spar and semisubmersible and in same environmental loads in order to generate data on coupled motions and loads between three platforms and investigate advantageous and disadvantageous of each platforms (Koo et al. 2014). A scaled model of NREL 5 MW wind turbine on three different platforms of TLP, spar and semisubmersible have been experimentally studied in a large number of tests so as to study the coupled system behavior of the three floating wind turbines subjected to combined wind and wave environmental loads. The results have demonstrated the unique advantages and disadvantages of each floating wind turbine platform (Goupee et al. 2014). The coupling effects created by changes in the hydrodynamic behavior of a semisubmersible FOWT have been investigated when it subjected to large inclinations under wind loads (Antonutti et al. 2016). They numerically have shown that the hull geometric nonlinearity effect and the alteration of viscous hydrodynamic forces can affect the dynamics of a typical FOWT operating in waves at rated conditions.

Dynamic response of a 1:50 scaled-down model of OC3 spar FOWT has been experimentally investigated (Duan et al. 2016). In the mentioned research, wind turbine blades could freely rotate without any undesirable effect of controlling wind turbine rotational speed.

A time domain numerical model of a braceless semisubmersible FOWT has been calibrated against experimental data of a 1:30 scaled model tested at MARINTEK's ocean basin (Berthelsen et al. 2016). Actually good agreements between simulations and experiments have been obtained by adjustment the numerical model. This adjustment was mainly related to the viscous drag coefficient on the platform's columns and pontoons.

There is a little research on the topic of experimental study on gyroscopic effect of revolving blades of a TLP FOWT on the structure motions. In this regard, the objective of this research is experimental investigation on the gyroscopic effect of rotating rotors and different wind heading angles on response of a TLP FOWT. In the current research, we have attempted to apply different environmental loads, consist of wave and wind with different headings, on the scaled FOWT and obtain the responses of the model in six DOFs. Analyzing the results has given us some notable information about effect of wind heading and rotor rotation speeds on the response of the structure.

Materials and methods

Characteristics of the TLP FOWT

In this research, the platform of the FOWT has been a sea star TLP and consisted of a single column equipped with four spokes which have hold four vertical tendons. This type of TLP platforms has been widely used in recent studies (Ren et al. 2012a, b; Pinkster 1980; Gueydon et al. 2014). But in this research the system has been stiffed in

the vertical direction much more than other typical TLPs. Due to the fact that for a model with this dimension no perfect tendons has been found. In this regard, the mentioned TLP has been restrained in the vertical direction as much as fixed platforms. Picture of the model installed to the tank is presented in Fig. 1. The main geometric parameters of the model have been demonstrated in Table 1. The information about the added mass, added inertia and hydrostatic stiffness of the platform which have been represented in Table 1, have been calculated by using former studies (Bachynski 2014; Karimirad et al. 2011).

Methods of obtaining gyroscopic effect

FOWTs work by gaining wind and rotation of their rotors. Rotation of rotors causes gyroscopic effect on the structure. The gyroscopic effect has been defined by Shilovskii: any couple, apparently tending to incline the axis of the rotating body in a given direction, actually causes an inclination of the axis in the plane perpendicular to that given direction (Shīlovskiĭ 1924; Gray 1918). The gyroscopic effect will be

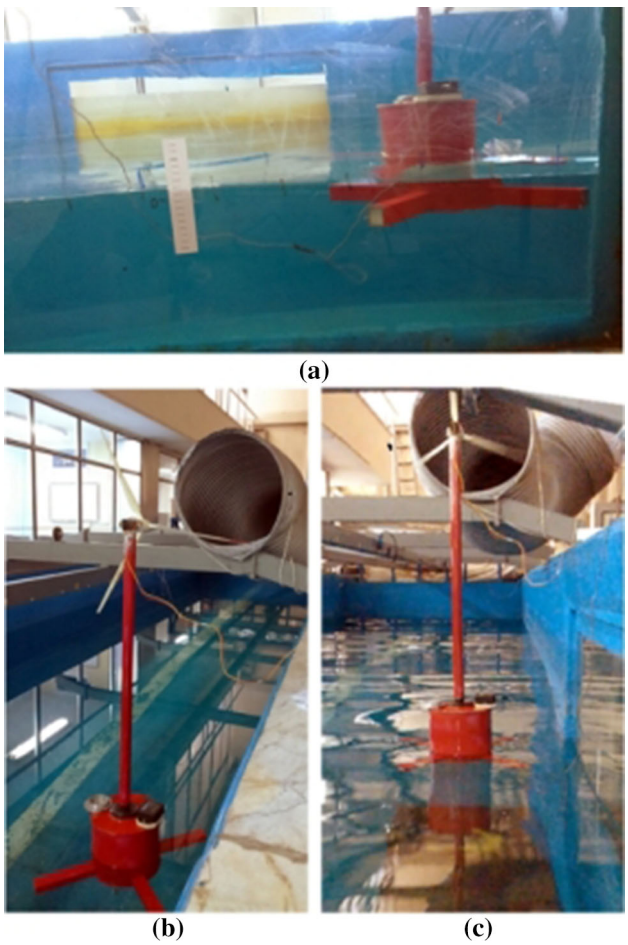

Fig. 1 **a** Tensioned legs of model, **b** model installed in the tank, **c** model subjected in wave and wind loads

in every system which has a revolving part. Equation of motion of the TLP FOWT can be driven from Newton's second law, and written as below:

$$F(t) = ([M] + [A])\ddot{x} + \left([C] + \left[C_g\right]\right)\dot{x} + [k]x \tag{1}$$

where $[M]$, $[A]$, $[C]$ and $[k]$ are, respectively, mass matrix, added mass matrix, damping matrix and total stiffness matrix and $F(t)$ is environmental loads applied to the structure which consists of wave, wind and aerodynamic loads. Also, $\left[C_g\right]$ is damping matrix which is caused by revolving of rotors (Fujiwara et al. 2011; Blusseau and Patel 2012). As respect to past studies, an operating wind turbine will induce extra damping (in rotational degrees of freedom except the one is align to the turbine's axis) and this extra damping can be defined by use of gyroscopic reaction moment using d'alembert principle:

$$L_p = I_p\omega_p \times i_p \tag{2}$$

where I_p is angular momentum, ω_p is constant rotation velocity and L_p is gyroscopic reaction moment.

$$-\frac{\mathrm{d}L_p}{\mathrm{d}t} = -I_p\omega_p \times \frac{\mathrm{d}i_p}{\mathrm{d}t} = -I_p\omega_p\Omega \times i_p \tag{3}$$

In above equation, Ω is angular velocity vector and can be expressed as below (Fujiwara et al. 2011):

$$\Omega \approx \mathrm{Re}\left\{-i\omega(X_4, X_5, X_6)\mathrm{e}^{-i\omega t}\right\} \tag{4}$$

where X_4, X_5, X_6 are, respectively, the rotational angles about x, y, z axes according to Fig. 2a. And ω the circular frequency of body motion equal to one of the incident wave.

Finally by substitution Eqs. 4 in 3, the following equation will be formed.

$$-\frac{\mathrm{d}L_p}{\mathrm{d}t} = -I_p\omega_p\mathrm{Re}\left\{-i\omega(X_4, X_5, X_6)\mathrm{e}^{-i\omega t}\right\} \times i_p \tag{5}$$

In the case of horizontal axis wind turbines, the unit vector is $i_p = (1, 0, 0)$ and former equation can be represented as the following form:

$$-\frac{\mathrm{d}L_p}{\mathrm{d}t} = I_p\omega_p\omega\mathrm{Re}\left\{i(0, X_6, -X_5)\mathrm{e}^{-i\omega t}\right\} \tag{6}$$

Equation 6 expresses the relation between rotation of rotating object and damping term in the equation of motion. Equation 7 shows the mentioned gyroscopic damping coefficient matrix.

$$C_g = \frac{I_p\omega_p}{\rho g} \times \begin{bmatrix} 0 & 0 & 0 & 0 & 0 & 0 \\ 0 & 0 & 0 & 0 & 0 & 0 \\ 0 & 0 & 0 & 0 & 0 & 0 \\ 0 & 0 & 0 & 0 & 0 & 0 \\ 0 & 0 & 0 & 0 & 0 & -1 \\ 0 & 0 & 0 & 0 & 1 & 0 \end{bmatrix} \tag{7}$$

Table 1 Characteristics of the platform and mooring lines

Parameter	Full scaled	Scale factor	Scaled model
Cylinder radius (m)	10	λ	0.10
Cylinder height (m)	20	λ	0.20
Total weight (kg)	2,500,000	λ^3	2.50
Total buoyancy (kg)	4,000,000	λ^3	4.00
Design depth (m)	100	λ	1
Hub diameter (m)	3	λ	0.03
Rotor diameter (m)	60	λ	0.60
Hub height (m)	90	λ	0.90
Characteristics of the mooring lines			
Vertical distance of cable	90	λ	0.90
Cable area (m^2)	3.8 E−3	λ^2	3.8 E−7
Cable young module (N/m^2)	1.99 E+13	λ	1.99 E+11
Pretension (N)	3.08E+7	λ^3	30.80
Unstretched length (m)	89	λ	0.89
Hydrostatic characteristics of the platform			
A_{11} (kg)	2.45	λ^3	2,450,560
A_{33} (kg)	1.59	λ^3	1,592,786.7
I_{55} (kg)	1000	λ^4	1e9
I_{xx}–I_{yy}	3.75 E+9	λ^5	0.375
I_{zz}	2.14 E+8	λ^5	0.0214
$k_{h\ \text{platform}}$ (N/m)	308.03	λ^2	3,080,340
$k_{p\ \text{platform}}$ (N/m)	2.45	λ^2	2,450,560

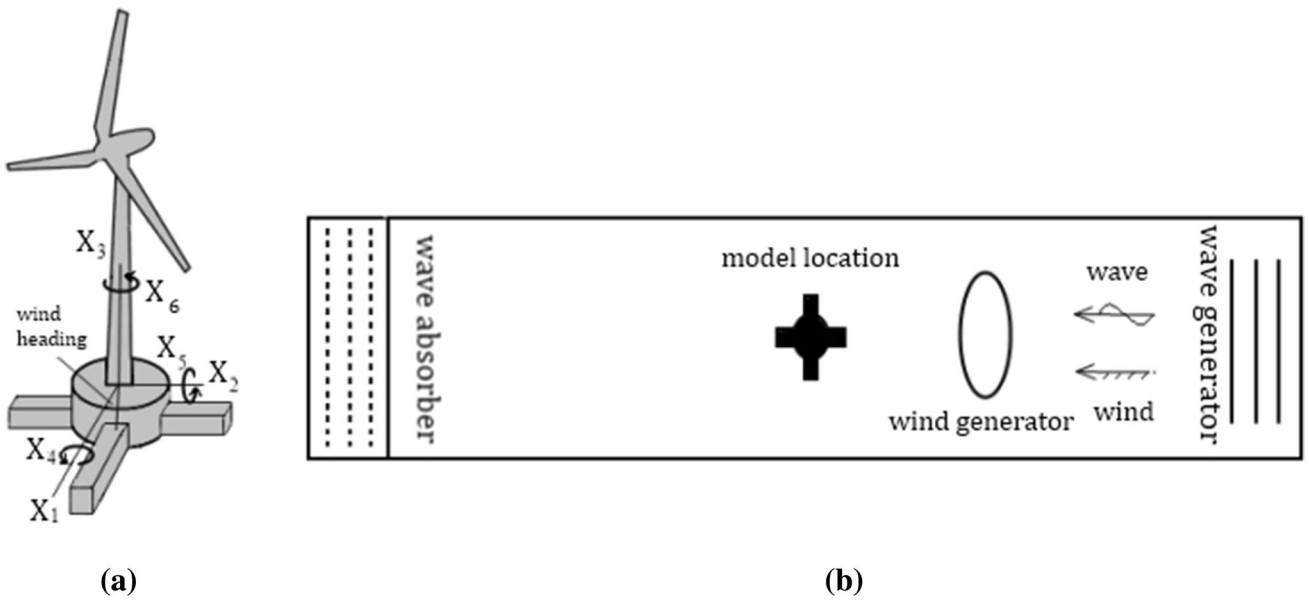

Fig. 2 **a** Coordinate system of FOWT, **b** a sketch of experimental setup of test in plane view

By inserting this gyroscopic damping term in Eq. 1 and rearranging it, the following form of equation of motion can be obtained.

$$F(t) = ([M] + [A])\ddot{x} + [k]x + \left([C] + \frac{I_p \omega_p}{\rho g} \times \begin{bmatrix} 0 & 0 & 0 & 0 & 0 & 0 \\ 0 & 0 & 0 & 0 & 0 & 0 \\ 0 & 0 & 0 & 0 & 0 & 0 \\ 0 & 0 & 0 & 0 & 0 & 0 \\ 0 & 0 & 0 & 0 & 0 & -1 \\ 0 & 0 & 0 & 0 & 1 & 0 \end{bmatrix} \right) \begin{bmatrix} \dot{x}_1 \\ \dot{x}_2 \\ \dot{x}_3 \\ \dot{x}_4 \\ \dot{x}_5 \\ \dot{x}_6 \end{bmatrix} \tag{8}$$

From Eq. 8, it can be concluded that gyroscopic damping coefficient is proportional to moment of inertia and velocity of rotation of the revolving part. Consequently, the rotation of the blades can influence response of the structure due to the mentioned extra damping term.

Methods of calculating natural frequency of the system

The natural frequency of each motion for the TLP FOWT can be defined as below (Shīlovskīĭ 1924):

$$\omega_n = \sqrt{\frac{k}{M + A}} \tag{9}$$

where k is stiffness in the specified motion, M is the mass and A is added mass in the mentioned motion. The equation can be extended for heave, surge, and pitch motions as below.

$$\omega_{\text{Surge}} = \sqrt{\frac{k_{\text{Surge}}}{M + A_{11}}} \tag{10}$$

$$k_{\text{Surge}} = k_{\text{stether}} = 4 \times \frac{T_0}{L} \tag{11}$$

where ω_{Surge} is the natural frequency in surge motion, k_{Surge} is total stiffness for surge motion, A_{11} is the surge added mass, k_{stether} is stiffness of each tether in surge motion, T_0 is the pretension of each tether and L is length of the tethers.

$$\omega_{\text{heave}} = \sqrt{\frac{k_{\text{heave}}}{M + A_{33}}} \tag{12}$$

$$k_{\text{heave}} = k_{h\,\text{platform}} + k_{h\,\text{tether}} \tag{13}$$

$$k_{h\,\text{platform}} = \rho g A_c \tag{14}$$

$$k_{h\,\text{tether}} = 4 \times \frac{A_t E}{L} \tag{15}$$

In above equations, ω_{heave} is the natural frequency for heave, $k_{h\,\text{platform}}$ is heave hydrostatic stiffness, $k_{h\,\text{tether}}$ is the tether stiffness for heave motion, A_{33} is the heave added mass, A_c is area of the platform in the water level, ρ is the water density, g is the gravity acceleration, A_t is tether section area and E is the elasticity modulus of the tethers.

$$\omega_{\text{Pitch}} = \sqrt{\frac{k_{\text{Pitch}}}{I_p + I_{55}}} \tag{16}$$

$$k_{\text{Pitch}} = k_{p\,\text{platform}} + k_{p\,\text{tether}} \tag{17}$$

$$k_{p\,\text{platform}} = \rho g \nabla \text{KB} - Mg\text{KG} + \rho g I \tag{18}$$

$$k_{p\,\text{tether}} = \frac{T_0}{L}(\text{KG} + L)\text{KG} \tag{19}$$

where ω_{Pitch} is the natural frequency for pitch, I_p and I_{55} are, respectively, pitch inertia and added pitch inertia, $k_{p\,\text{platform}}$ is pitch hydrostatic stiffness, $k_{p\,\text{tether}}$ is the tether stiffness for pitch motion, A_{55} is the pitch added mass, ∇ is the submerged volume, KB and KG are, respectively, distance of the center of buoyancy and center of gravity from bottom of the platform and I is the area moment of inertia.

According to all characteristics which have been represented in the Table 1 and all mentioned equations, the natural frequencies of the system have been calculated as below.

$$\omega_{\text{Surge}} = 0.52 \tag{20}$$

$$\omega_{\text{Heave}} = 28.29 \tag{21}$$

$$\omega_{\text{Pitch}} = 0.33 \tag{22}$$

Methods of calculating second-order wave loads

For calculating both sum and diffraction frequency second-order loads on the TLP FOWT, the pressure integration approach has been used and according to former studies, the equation of sum-frequency second order has been represented as the following form (Chen and Molin 1990):

$$\overrightarrow{F_{22}(2\omega)} = 2i\omega \frac{\rho}{g} \iint_{z=0} a_D . \Phi_R(2\omega) \mathrm{d}S \tag{23}$$

where F_{22} is the exciting force, a_D is the right-hand side of free surface equation and Φ_R is radiation potential at the double frequency, 2ω. The equation of diffraction frequency second order has been represented as below (Pinkster 1980; Gueydon et al. 2014):

$$\begin{aligned} \overrightarrow{F_{(2)}} = {} & \frac{1}{2}\rho g \iint_{\text{W.L.}} \zeta^2_{(1)\cdot\text{rel}} \cdot \vec{n_0} \cdot \vec{\mathrm{d}l} + \frac{1}{2}\rho \iint_S \nabla\phi_{(1)} \cdot \nabla\phi_{(1)} \cdot \vec{n_0} \mathrm{d}S \\ & + \iint_S \rho X_{(1)} \cdot \nabla \frac{\partial \phi_{(1)}}{\partial t} \cdot \vec{n_0} \mathrm{d}S + \overrightarrow{\Omega_{(1)}} \times M \cdot \overrightarrow{X_{(1)}} \\ & - \rho \iint_S \frac{\partial \phi_{(2)}}{\partial t} \cdot \vec{n_0} \mathrm{d}S \end{aligned} \tag{24}$$

Rotor speed (rpm)	Wind angle: 0'						Wind angle: 90'					
	Heave		Surge		Pitch		Heave		Surge		Pitch	
	Max(m)	Std	Max(m)	Std	Max(m)	Std	Max(m)	Std	Max(m)	Std	Max(m)	Std
0	0.247	0.09	7.085	3.69	3.62	1.40	0.257	0.09	7.223	3.67	3.82	1.61
30	0.271	0.10	6.009	3.61	4.31	1.81	0.271	0.0913	6.771	3.60	4.01	1.84
60	0.358	0.11	6.211	3.56	3.89	1.67	0.222	0.063	6.778	3.69	4.17	1.71

(a)

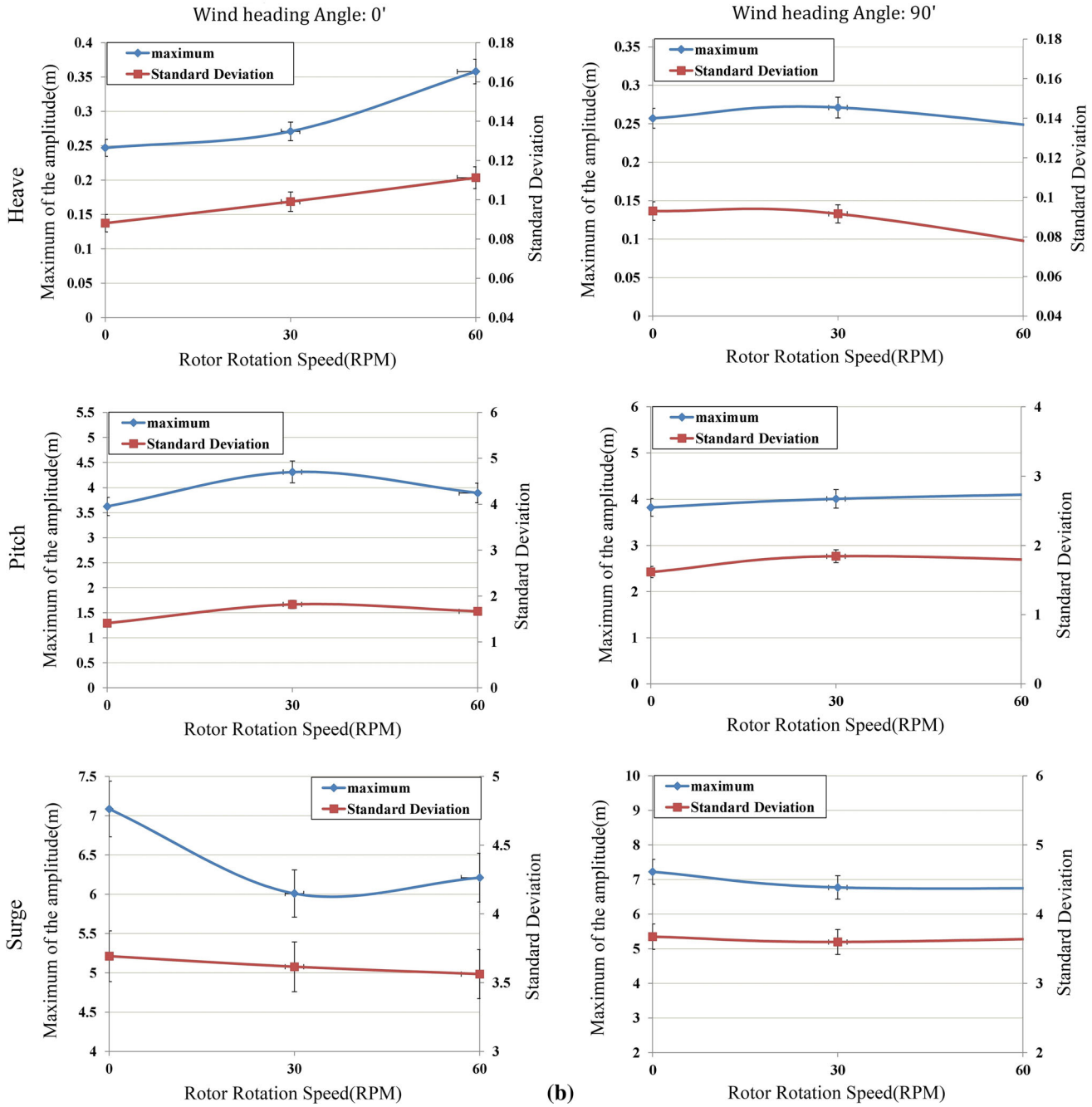

Fig. 3 **a** Table of maximum amplitude and STD in three different rotor rotation speeds, **b** maximum amplitude and standard deviation for heave, surge and pitch in three different rotor rotation speed and two different wind angle

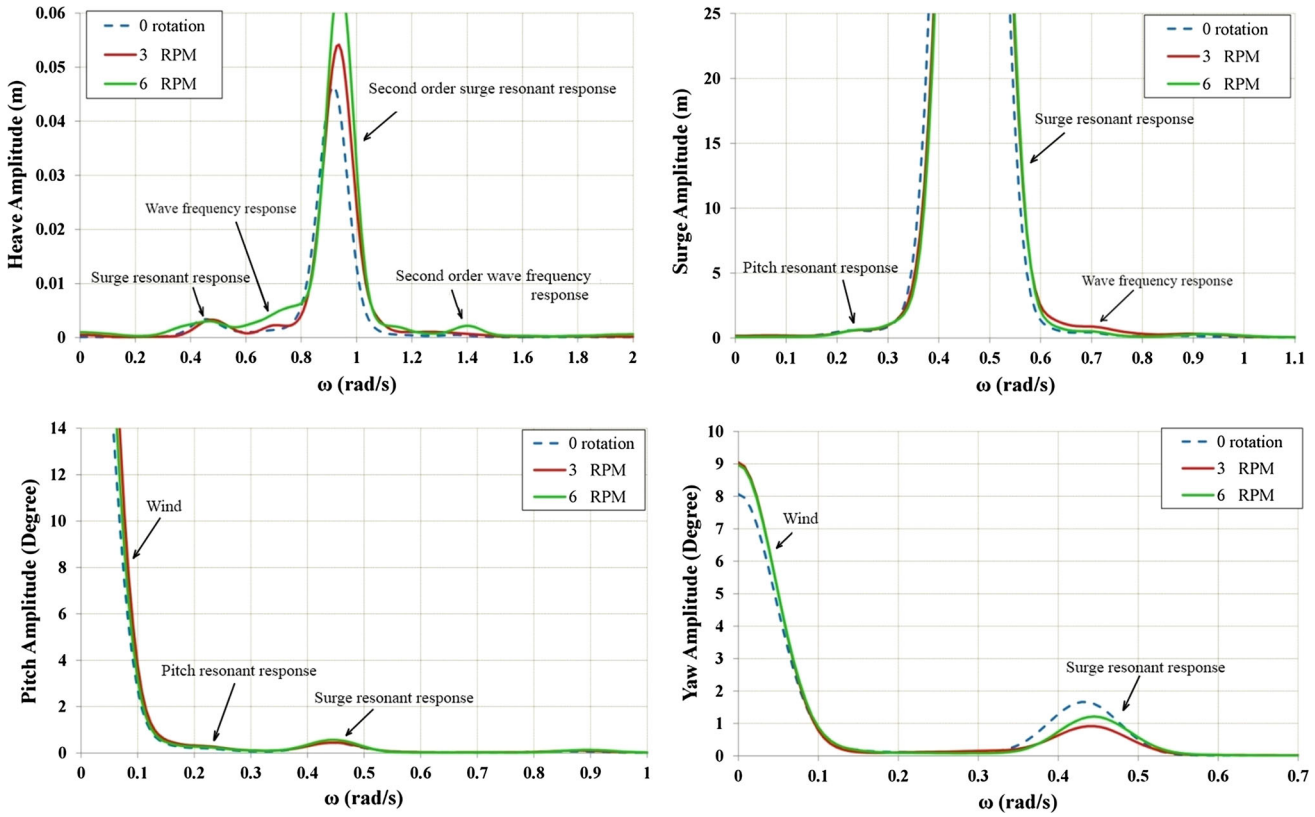

Fig. 4 Response spectra for heave, pitch and surge for three different rotor rotation velocities

In the above equation, Subscript (1) denotes when a quantity is of the first order and (2) denotes when a quantity is of the second order. And $\zeta_{.\mathrm{rel}}$ is relative wave elevation, W.L. is water line, n_0 is the outward pointing normal vector, dl is element of water line vector, ϕ is the velocity potential, dS is the surface element of the wetted hull and Ω is the angular motion vector.

Wave-wind tank

The experiment has been carried out in the Marine laboratory of Sharif University. The tank dimension is 22.5 m × 2.5 m with the depth of 1.2 m. The paddle-type wave generator is able to generate waves with the height range of 0.01–0.08 m and 0.5–1.5 s periods (Sarlak et al. 2010). The wind generator consists of an axial fan and an inverter in order to control the input electric current, rotational speed of fan's blades and consequently, the output wind speed. The wind generator is able to generate a maximum wind speed of 30 m/s. A schematic of the experimental setup of test is shown in Fig. 2b.

The wind generator is stand on its legs which are out of the tank and the generated wind is guided to the model by a duct. The speed of the generated wind subjected to model has been measured during the tests by a wind speed meter with the accuracy of ±3% and measurement speed range of 0–30 m/s. The wind around the wind turbine has not been completely uniform and has had a little turbulent which has caused some negligible tower's oscillation. Due to low laboratory equipment, the generated wind has been considered as a uniform constant wind.

Actually, in order to rotate the blades and hub with the desired speed, a power supply and an armature has been utilized.

Scaled model

Platform design

In this research, a sea star TLP for depth of 100 m, have been designed as the platform of the FOWT. Actually, the structure has been consisted of a single column equipped with four spokes which have hold four vertical tendons. This type of TLP platforms has been widely used in recent studies (Ren et al. 2012a, b; Pinkster 1980; Gueydon et al. 2014). The Froude-scaled model of the TLP FOWT has been fabricated in the marine Laboratory of Sharif University of Technology. The platform model has been constituted of a polycarbonate PVC cylinder and four aluminum alloy profiles for its spokes and they have been

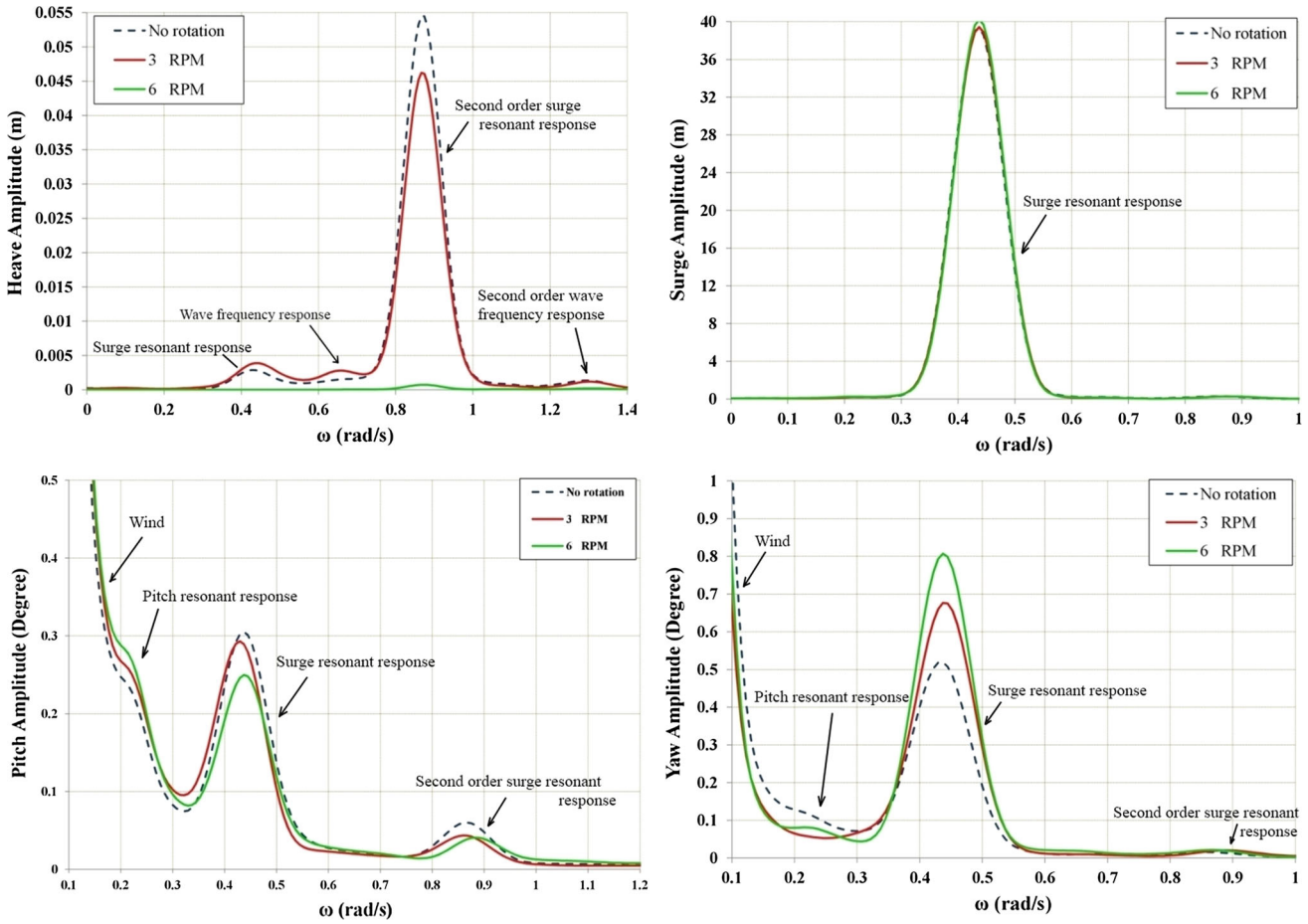

Fig. 5 Response spectra for heave, pitch and surge for three different rotor rotation velocities in 90° wind heading

latched to each other. The tower has been consisted of a PVC pipe with a hub and blades on its top and has been connected and fixed to the platform. The ratio of model to prototype is 1/100 based on the Froude Number (Crozier 2011; Chakrabarti 1998). This model has been tested in the towing tank of Sharif University in order to study the gyroscopic effects and the heading of wind on the platform response of FOWT, and obtaining spectrums of significant motions.

In order to make the model in detail and minimize the errors, a significant effort has been made and the model has been produced three times to have minimum error in geometry. In order to best assessment of center of gravity, weight of all components of the model has been measured and due to their location on the model, the center of gravity has been obtained.

Rotors and blades design

The hub and rotors have been scaled based on the Froude number (Chakrabarti 1998; Chanson 2004) and have been constructed with detail of 0.1 mm by a 3D printer. A particular care has been taken in selecting material and fabricating the blades. The blades and the hub have been latched to each other carefully without any slip.

Due to the friction between hub and connecting shaft to the tower, the rotors have not moved by blowing the wind to the model. Consequently, in this research the rotors have been revolved by a power supply and an armature. In this regard, the performance of the model has been different to the full-scaled wind turbine. But due to the lack of sufficient information about downstream wind, finding characteristics of the scaled rotors have become impossible.

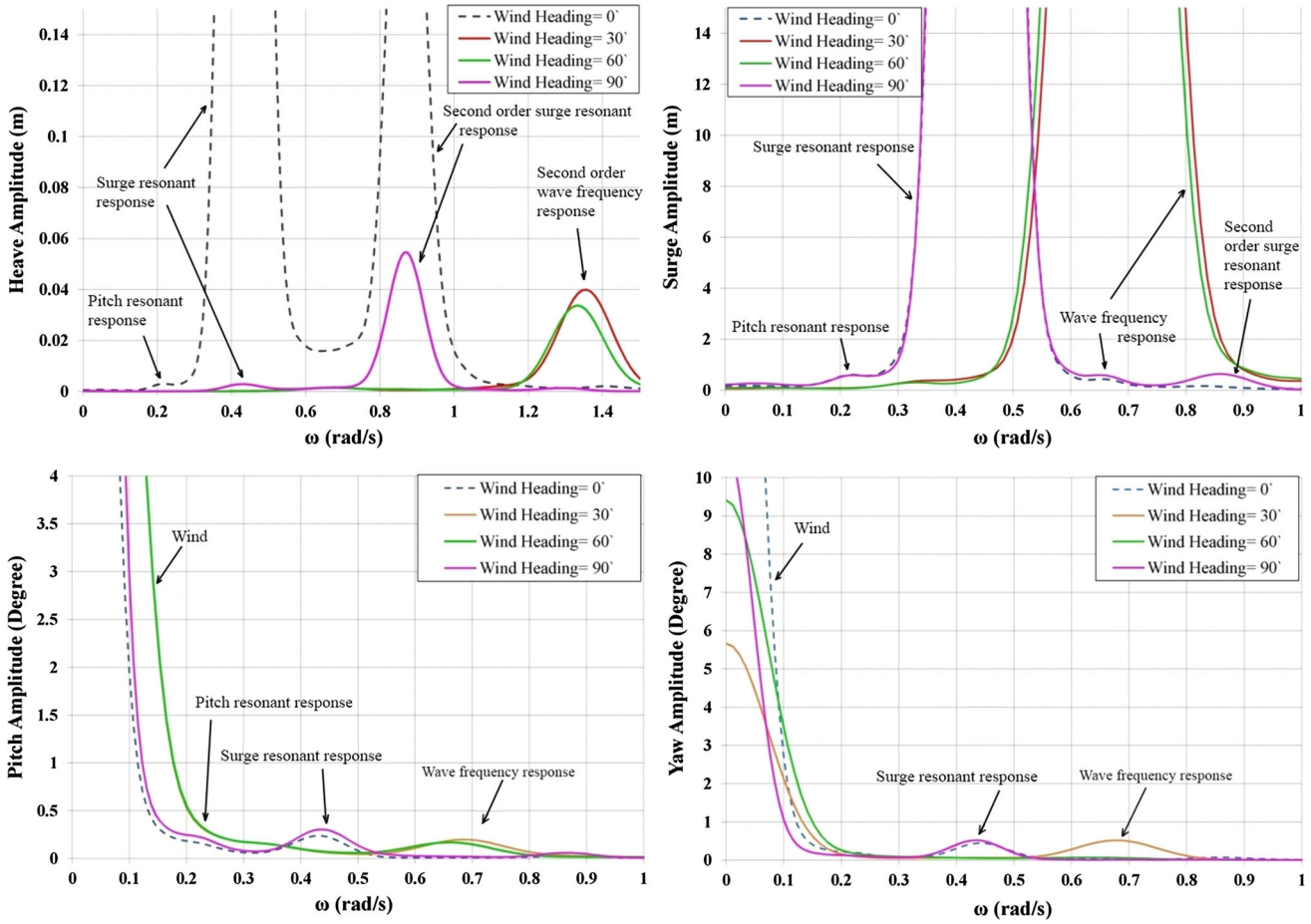

Fig. 6 Response spectra for heave, pitch and surge for four different wind headings without rotor rotation

Mooring line

As respect of enormous aerodynamic load acting on the turbine, the mooring system of the model has a significant importance on dynamic response of the platform. Since the mooring lines of the platform have been long slender bodies and their stiffness have played a significant role in their responses so the moorings have been scaled due to the Cauchy Number (Chanson 2004). The main parameters of the mooring system have been presented in the Table 1. In order to construct the mooring lines as accurately as possible, four steel wires which has had 0.7 mm diameter, have been used and connected to the model and bed of the tank.

Calibration and test condition

A notable number of tests have been performed so as to evaluate the gyroscopic effect and wind heading angle effect, on the different platform motions. In all the tests characteristics of the wind and wave have been scaled down by the Froude Number (Chakrabarti 1998; Chanson 2004). Consequently, three different scenarios have been pursued in this research. The first one is studying gyroscopic effect of rotor rotation speed on the structure responses. For this purpose, tests with same wave and wind characteristics and different in rotor rotation velocities have been performed.

The second scenario is obtaining effect of heading angle of wind on the structure responses. In this regard, tests with same characteristics and different wind headings, 0, 30, 60, 90 toward the model, have been carried out.

Finally, the last one is studying effect of different sea states on heave, surge and pitch motions. In order to do so, six different sea states have been applied to the model and their results have been captured and analyzed.

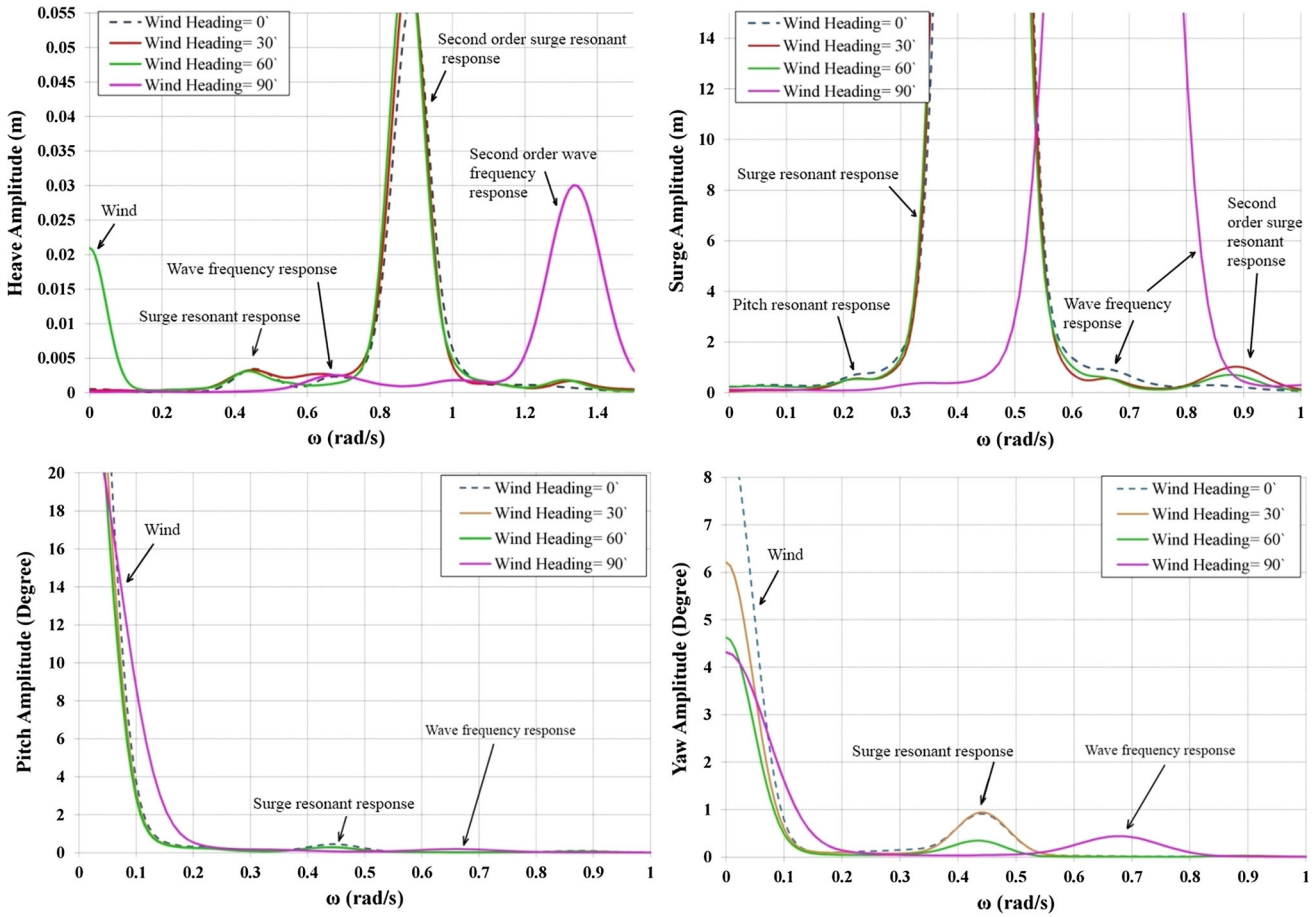

Fig. 7 Response spectra for heave, pitch and surge for four different wind headings with 30 rpm rotor rotation

Results and discussion

Gyroscopic effect of rotors rotation

An operating wind turbine has excited extra loads on the structure and it has leaded a change in spectrum of platform motions. For attaining effect of rotor rotation velocity on the structure responses, in a constant wave and wind loads, 3 different rotor rotation speeds, 0, 30 and 60 rpm have been applied to the model with constant regular wave with 0.03 m height and 1 s period. This set of tests has been divided into two parts. In the first part, heading angle of wind related to the model was 0°. The result of tests has been scaled up and shown in Figs. 3b and 4.

By analyzing time response results, it can be deduced that the most sensitive motion to the rotor speed can be the heave motion in wind angle of 0′. Figure 3a represents the standard deviation and maximum amplitude of heave, surge and pitch motions in different rotor speeds. Also, these results are shown in Fig. 3b. Also, effect of wind can be seen in the pitch and yaw spectrum as well (Chanson 2004).

Besides, the experimental results have represented that in the heave, surge, pitch and yaw spectrums, rotation of rotors has shifted the peak of curve to a higher frequency due to the fact that rotation of blades has induced an extra damping in the equation of motion, which has been discussed in the theoretical background section in Eq. 8. Addition to this, amplifying of the peak in the heave spectrum can be seen as well.

In the next part of this section, the tests have repeated once again but in 90° wind heading angle for obtaining the result of structure responses in 90° angle of wind.

The results have shown that when the wind heading angle is 90° the movement of peak observed in the last part, has become very slight. In the heave spectrum, the curve for 60 rpm rotation speed has tended to a horizontal line (Fig. 5).

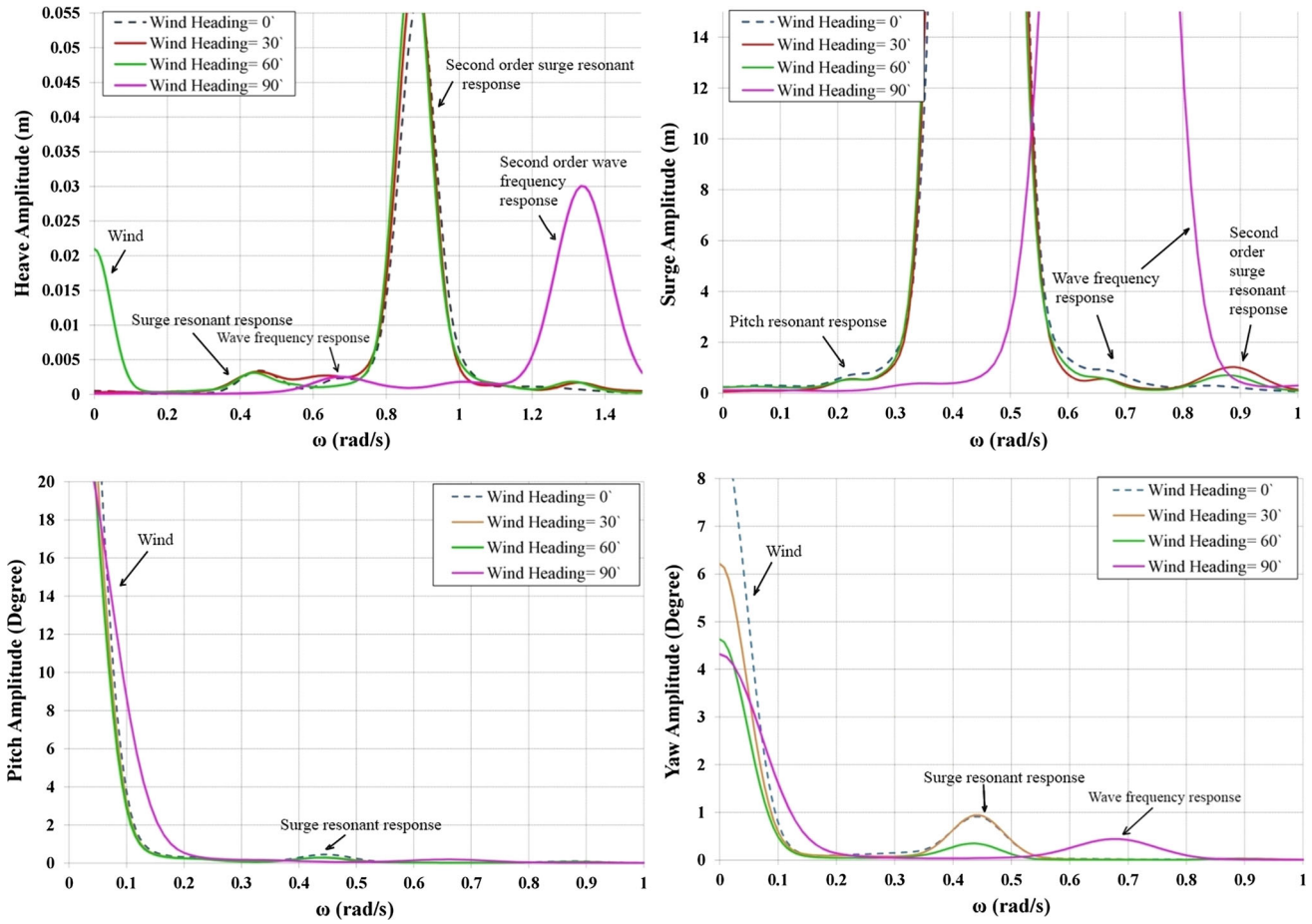

Fig. 8 Response spectra for heave, pitch and surge for four different wind headings with 60 rpm rotor rotation

Also, in the mentioned figures in this section, double frequencies of wave and surge motion which have been induced according to Eqs. 23 and 24 can be observed.

Effect of wind heading on structure responses

For studding the effect of wind heading angle on the structure responses, in a constant wave and wind loads, four different wind heading angles, 0°, 30°, 60° and 90° have been applied to the model with constant regular wave with 0.03 m height and 1 s period. Actually, this section has been divided into three parts which have been distinguished from each other by the speed of rotor criteria.

In the first part of this section, tests with no rotor rotation have been carried out. The results have demonstrated that heave and yaw behavior in 0° and 90° wind headings have been similar and on the other hand, the 30° and 60° headings have done so. And in the surge and pitch, the 30° and 60° headings have been shifted to higher frequency (Fig. 6).

In the next part, the mentioned tests have been done with 30 rpm rotor rotational speed. Figure 7 shows the structure spectrums for these tests. In the heave and surge spectrums, all headings except 90° heading have had the same behavior. But in the pitch and yaw, spectrums all headings have been similar to each other.

In the last part of this section, tests have been carried out with 60 rpm rotor rotation speed. In the heave spectrum just 0 wind heading curve have been distinct from other headings. In the surge, pitch and yaw spectrums similarity between 0° and 90°, and between 30° and 60° wind heading curves have been observed (Fig. 8).

Test No.	wave height (m)	wind speed (m/s)	rotor speed (rpm)
1	0.03	10	3
2	0.03	20	6
3	0.04	30	6
4	0.045	40	6
5	0.05	50	6
6	0.06	60	6

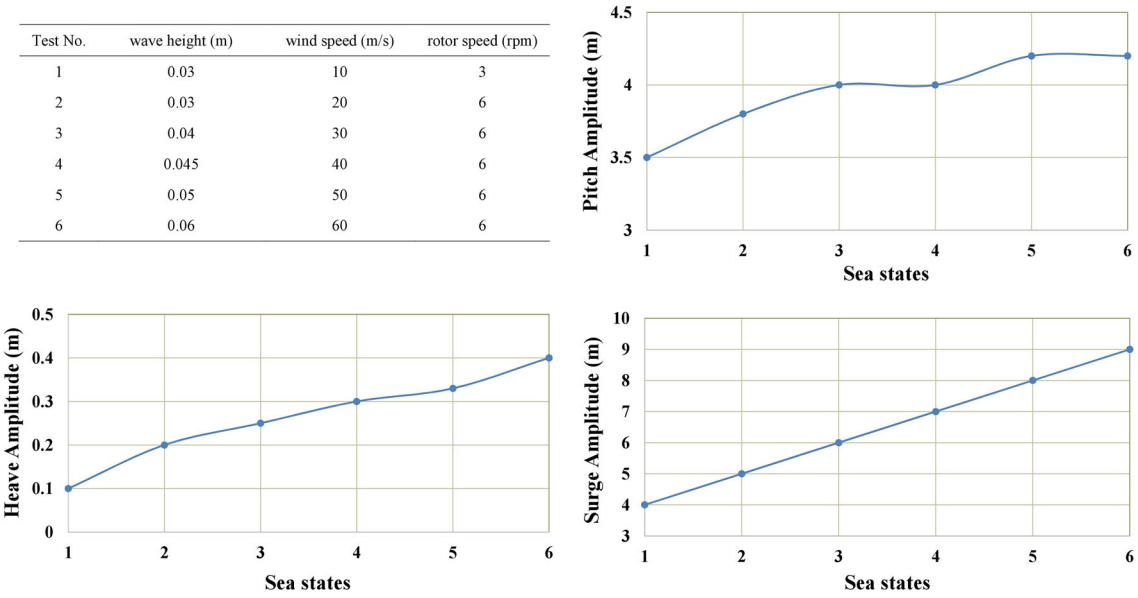

Fig. 9 Heave, surge and pitch amplitude in different sea states

Effect of different sea states on structure responses

In order to study on effect of different sea states on the structure motions, six different sea states have been specified and applied to the model. The results of the heave, surge and pitch motions are acquired and represented in Fig. 9. The results have expressed that heave and surge are the most sensitive motions to the sea states. By applying more rough conditions, the heave and surge amplitudes can reach as high as four times of their amplitudes in the most slight condition.

Conclusion

This research has presented an experimental investigation on gyroscopic effect and effect of wind heading angle on the structure responses. Some equations which have represented the relation between gyroscopic effect and response of the structure have been taken into account. Consequently, three sets of tests have been performed. The first one has been divided into two parts. In the first part, model has been subjected to the constant wave and wind loads with 0 angle heading, but different blade rotation velocities. The results have expressed that rotation of the blades has shifted the peak of heave, surge, pitch and yaw spectrums to a higher frequency due to additional gyroscopic damping matrix which has been induced. And the peak of heave spectrum has been amplified by revolving the blades.

In the second part only wind heading angle has been changed to 90° and the results have shown that the shifting of the peak due to revolving blades, have become very slight and the mentioned amplification of the peak can be observed only in the yaw spectrum.

In the second set of tests, the effect of wind heading on the structure has been investigated. In order to do so, tests have been carried out in different four angles of wind, three times with three different rotational speeds of blades.

In the no rotation, the results have demonstrated that structure in the 30° and 60° of wind heading angle has had the same behavior and the structure in 0° and 90° of wind angles has done so.

But when the mentioned tests have been repeated in 30 and 60 rpm rotor rotation velocities, the results have become different. In the 30 rpm rotating speed, only curve of 90° wind heading have been distinguished from the curves with other wind heading angles. In the 60 rpm tests, only the 0 wind heading curve has differed to others in heave motion. In surge, pitch and yaw motions similarity between 0° and 90°, and between 30° and 60° wind heading curves can be observed.

In the heave spectrum just 0 wind heading curve has been distinct from others. In the surge, pitch and yaw

spectrums the 0° and 90°, and between 30° and 60° wind heading curves have had same behavior as well as first part of this section.

Finally, in the last part of the research, effect of different sea states on the heave, surge and pitch motions has been studied. It has been observed that the most sensitive motions to the sea states are heave and surge motions.

By taking into account all above-mentioned observations, it can be concluded that rotation of blades of a FOWT can affect position of the peak of spectrums but inclination of wind heading may reduce it. Actually, wind heading angle may change behavior of spectrums which can be affected by rotor velocity as well.

Acknowledgement The authors want to thank staff of Marine laboratory of Sharif University of Technology for helping producing the model and accomplishing tests.

References

Antonutti R, Peyrard C, Johanning L, Incecik A, Ingram D (2016) The effects of wind-induced inclination on the dynamics of semi-submersible floating wind turbines in the time domain. Renew Energy 88:83–94

Bachynski EE (2014) Design and dynamic analysis of tension leg platform wind turbines, Doktoravhandlinger ved NTNU, 1503-8181; 2014:86, PhD thesis, NTNU, Trondheim, Norway

Bagbanci H (2011) Dynamic analysis of offshore floating wind turbines. Naval Architecture and Marine Engineering, Technical University of Lisbon

Berthelsen PA, Bachynski EE, Karimirad M, Thys M (2016) Real-time hybrid model tests of a braceless semi-submersible wind turbine. Part III: calibration of a numerical model. In: Proceedings of the ASME 2016 35th international conference on ocean, offshore and arctic engineering OMAE2016 June 19–24, 2016, Busan, Korea

Blusseau P, Patel MH (2012) Gyroscopic effects on a large vertical axis wind turbine mounted on a floating structure. Renew Energy 46:31–42

Browning JR, Jonkman J, Robertson A, Goupee AJ (2014) Calibration and validation of a spar-type floating offshore wind turbine model using the FAST dynamic simulation tool. In: Journal of physics: conference series, vol. 555, no. 1. IOP Publishing, p 012015

Chakrabarti S (1998) Physical model testing of floating offshore structures. In: Dynamic positioning conference

Chanson H (2004) Hydraulics of open channel flow. Butterworth-Heinemann, Oxford

Chen XB, Molin B (1990) High frequency interactions between TLP legs. In: 5th international workshop on water wavesand floating bodies

Crozier A (2011) Design and dynamic modeling of the support structure for a 10 MW offshore wind turbine, MSc thesis, NTNU, Trondheim, Norway

Duan F, Hu Z, Niedzwecki JM (2016) Model test investigation of a spar floating wind turbine. Mar Struct 49:76–96

Ebrahimi A, Abbaspour M, Nasiri RM (2014) Dynamic behavior of a tension leg platform offshore wind turbine under environmental loads. Sci Iran Trans A Civ Eng 21(3):480

Fujiwara H, Tsubogo T, Nihei Y (2011) Gyro effect of rotating blades on the floating wind turbine platform in waves. In: The twenty-first international offshore and polar engineering conference. International Society of Offshore and Polar Engineers

Goupee AJ, Koo BJ, Kimball RW, Lambrakos KF, Dagher HJ (2014) Experimental comparison of three floating wind turbine concepts. J Offshore Mech Arct Eng 136(2):020906

Gray A (1918) A treatise on gyrostatics and rotational motion: theory and applications. Macmillan and Company limited, New York

Gueydon S, Duarte T, Jonkman J (2014) Comparison of second-order loads on a semisubmersible floating wind turbine. In: ASME 2014 33rd international conference on ocean, offshore and arctic engineering. American Society of Mechanical Engineers, pp V09AT09A024–V09AT09A024

Hsu WY, Yang RY, Chang FN, Wu HT, Chen HH (2016) Experimental study of floating offshore platform in combined wind/wave/current environment. Int J Offshore Polar Eng 26(02):125–131

Jonkman JM (2007) Dynamics modeling and loads analysis of an offshore floating wind turbine. ProQuest, Ann Arbor

Karimirad M, Meissonnier Q, Gao Z, Moan T (2011) Hydroelastic code-to-code comparison for a tension leg spar-type floating wind turbine. Mar Struct 24(4):412–435

Koo BJ, Goupee AJ, Kimball RW, Lambrakos KF (2014) Model tests for a floating wind turbine on three different floaters. J Offshore Mech Arct Eng 136(2):020907

Martin HR, Kimball RW, Viselli AM, Goupee AJ (2012) Methodology for wind/wave basin testing of offshore floating wind turbines. In: Proceedings of the ASME

Matha D (2010) Model development and loads analysis of an offshore wind turbine on a tension leg platform with a comparison to other floating turbine concepts: April 2009 (No. NREL/SR-500-45891). National Renewable Energy Laboratory (NREL), Golden

Matha D, Schlipf M, Pereira R, Jonkman J (2011) Challenges in simulation of aerodynamics, hydrodynamics, and mooring-line dynamics of floating offshore wind turbines. In: The twenty-first international offshore and polar engineering conference. International Society of Offshore and Polar Engineers

Naqvi SK (2012) Scale model experiments on floating offshore wind turbines. Doctoral dissertation, Worcester Polytechnic Institute

Pinkster JA (1980) Low frequency second order wave exciting forces on floating structures. Doctoral dissertation, TU Delft, Delft University of Technology

Ren N, Li Y, Ou J (2012a) The effect of additional mooring chains on the motion performance of a floating wind turbine with a tension leg platform. Energies 5(4):1135–1149

Ren N, Li Y, Ou J (2012b) The wind-wave tunnel test of a new offshore floating wind turbine with combined tension leg-mooring line system. In: The twenty-second international

offshore and polar engineering conference. International Society of Offshore and Polar Engineers

Sarlak H, Seif MS, Abbaspour M (2010) Experimental investigation of offshore wave buoy performance. Int J Marit Technol (IJMT) 6(11):1–11

Shīlovskīĭ PP (1924) The gyroscope: its practical construction and application: treating of the physics and experimental mechanics of the gyroscope, and explaining the methods of its application to the stabilization of monorailways, ships, aeroplanes, marine guns, etc. E. & FN Spon, Limited, London

Shin H (2011) Model test of the OC3-Hywind floating offshore wind turbine. In: The twenty-first international offshore and polar engineering conference. International Society of Offshore and Polar Engineers